

Effects of real environments on the performance of quantum Lidar

Wang Qiang¹, Hao Lili¹, Tang Hongxia², Li Xianli¹, Mu Haiwei¹, Han Lianfu¹, Zhao Yuan³

(1. Department of Physics, Northeast Petroleum University, Daqing 163318, China;

2. College of Electrical Engineering, Suihua University, Suihua 152000, China;

3. Department of Physics, Harbin Institute of Technology, Harbin 150001, China)

Abstract: The effects of loss and noise (real environments) on the performance of quantum lidar with odd coherent superposition states source (OCSR) was investigated. The general expression of conditional probabilities and parity photon counting measurement strategies were exploited to derive the mean value of the output signal and its phase sensitivity from the Mach-Zehnder interferometer (MZI). It can be found from the output signal that loss destroys the coherence and further descends the performance of lidar. The numerical calculation shows that the odd and even interference fringes emerge in the whole interference pattern, and the odd interference term which represents the coherence is extremely sensitive to particle loss. The odd coherent states quantum lidar outperforms the performance achieved by the traditional coherent states (CS) lidar only in small loss regimes. However, in the noisy environments, OCSR gives the better resolution and sensitivity than CS in the regions of $\kappa > 0.3$ and $\kappa > 0.06$, respectively.

Key words: Lidar; quantum optics; Rayleigh diffraction limit; super-resolution

CLC number: O43; TN249 **Document code:** A **DOI:** 10.3788/IRLA201847.S106006

实际环境对量子激光雷达性能的影响

王 强¹, 郝利丽¹, 唐红霞², 李贤丽¹, 牟海维¹, 韩连福¹, 赵 远³

(1. 东北石油大学 物理系, 黑龙江 大庆 163318; 2. 绥化学院 电气工程学院, 黑龙江 绥化 152000;

3. 哈尔滨工业大学 物理系, 黑龙江 哈尔滨 150001;

摘 要: 研究了损耗和相位噪声对奇相干态(OCSR)量子激光雷达性能的影响。利用条件概率的一般表达式和奇偶光子计数探测方法推导了马赫-增德尔干涉仪(MZI)输出信号的平均值和相位灵敏度。从信号平均值的表达式中可以看出光子数损耗破坏了信号的相干性进而导致了激光雷达性能的下降。数值计算结果表明:输出信号的干涉花样中出现了奇偶相干项,且奇相干项对损耗及其敏感;系统的输出性能只有在小损耗区域内优于传统的激光雷达。而在噪声环境中,在噪声区域 $\kappa > 0.3$ 内,奇相干态的信号分辨率优于相干态,而在 $\kappa > 0.06$ 区域内,奇相干态的奇偶光子计数探测信号的灵敏度好于相干态。

关键词: 激光雷达; 量子光学; 瑞利衍射极限; 超分辨率

收稿日期:2018-02-15; 修订日期:2018-05-11

基金项目:东北石油大学青年科学基金(NEPUQN2015-1-12);东北石油大学国家自然科学基金培养基金(2017PYYL-07);

黑龙江省教育厅项目(12531838);国家自然科学基金(51374072, 51374072, 41472126)

作者简介:王强(1980-),男,博士生,主要从事量子干涉、度量和传感方面的研究。Email:wangqiang8035@163.com

导师简介:赵远(1963-),男,教授,博士生导师,主要从事激光雷达和光电信号检测等方面的研究。Email:zhaoyuan@hit.edu.cn

通讯作者:郝利丽(1981-),女,博士生,主要从事非线性光学和量子光学等方面的研究。Email:haolili0820@126.com

0 Introduction

Resolution and sensitivity are extremely important parameters for many fields of science and technology, these fields involve in quantum metrology, imaging, object ranging, quantum sensor and quantum radar or lidar^[1-4], to name a few. In a traditional coherent-light Mach-Zehnder interferometer(MZI), the resolution and sensitivity are known as the Rayleigh resolution limit and the shot-noise limit, respectively. The classical diffraction limit and shot-noise limit can be beaten by utilizing some non-classical states of light as the input of MZI. One of the most prominent examples of such a non-classical state is the $N00N$ state, which is an equal coherent superposition of N photons in one path of a MZI with none in the other, and vice-versa^[5-7]. However, due to inevitable interactions with the surrounding environment, the $N00N$ states tends to decohere in the presence of loss and noise, which makes it difficult to achieve super-sensitivity and super-resolution. In a lossy interferometer, it has been shown that a transition of the precision from the Heisenberg limit to the shot noise limit occurred with the increase of photon number N . All of these reveal that using such quantum states of light as the source of remote quantum sensor, such as quantum Radar or Lidar, has no advantages than the traditional Radar or Lidar.

Therefore, Gao and Jiang proposed a super-resolving quantum lidar scheme with coherent states (CS), photon-number-resolving detectors^[8] and quantum homodyne detection scheme^[9] to beat the classical diffraction limit. Coherent states of light can mitigate the super-Beer's law in photon loss and maximize sensitivity. Distant et al and Cohen et al. demonstrated the super-resolution with $\Delta x \propto \lambda/2N$ in a coherent light MZI and in a polarization version of the MZI, respectively^[10-11]. However, small noise had seriously declined the fringe resolution and the achievable phase sensitivity^[12]. The concept of coherent

state was first introduced by Glauber^[13], and since then attained an important position in the study of quantum optics. Based on this work, the odd coherent superposition states(OCSS) were introduced in Ref.[14]. Coherent superposition and anti-bunching are the main characteristics of OCSS relative to CS, which indicates OCSS possessing extensive application prospect.

We present a new Lidar scheme with odd coherent superposition states source in the presence of loss and phase noise in this manuscript. The binary-outcome photon counting data post processing methods are exploited to enhance the resolution and sensitivity. The effects of photon loss and phase noise on the output signal are all considered in the calculation. The numerical calculation manifests that the odd interference fringes appear in the interference pattern which means twofold super-resolution of OCSS compared to CS in lossless and noiseless cases. Little loss will drop the amplitude of odd interference peaks rapidly, whereas the amplitude of the even interference peak keeps invariability. With the loss further increasing, the odd interference peaks disappear, and the even interference peaks begin widening. Only in the small loss regions, OCSS coupled with the parity detection gives better resolution than that of CS, while the sensitivities of these two states are identical in the lossy environment. In addition, the effects of the phase noise on the output signals are emphasized. The numerical results show that OCSS gives better resolution and sensitivity than that of CS in the phase diffusion interval of $\kappa > 0.3$ and $\kappa > 0.06$, respectively.

1 Two-mode interferometric quantum Lidar scheme with odd coherent superposition states sources

Figure 1 illustrates the two-mode interferometric quantum Lidar scheme, which is consisted of a standard MZI fed with odd coherent superposition states of light, two fictitious beam splitters $\hat{B}(T)$ and a phase shifter(PS) $\Delta\varphi(t)$. Path a and b represent the

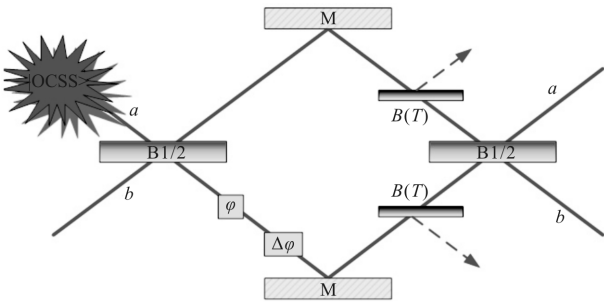


Fig.1 Scheme of a two-mode interferometric quantum lidar with OCSS

probe signal path and local signal path, respectively. An odd coherent superposition state is injected into one port of the MZI and the other port is left in vacuum $|0\rangle$. After passing through the first 50:50 beam splitter (BS1), the coherent superposition state is turned into $N_o(|i\alpha/\sqrt{2}\rangle|-\alpha/\sqrt{2}\rangle-|-i\alpha/\sqrt{2}\rangle|\alpha/\sqrt{2}\rangle)$ which is in fact an entangled coherent state. The roles of photon loss are described by introducing one fictitious beam splitter $\hat{B}(T)$ after the phase accumulation and phase-diffusion process. The fictitious beam splitter $\hat{B}(T)$ couples the interferometric mode a (or b) and the environment mode e with transmissivity T . The reflectivity corresponding to T is denoted as R . The state after BS1 will be further transformed by the phase shifter, the fictitious beam splitters and the second 50:50 beam splitter (BS2), thus, the result states can be written as

$$|\psi\rangle_{\text{out}} = N_o \left(|\beta \sin \frac{\varphi}{2}\rangle_a |-\beta \cos \frac{\varphi}{2}\rangle_b |-\gamma\rangle_{a'} |-i\gamma e^{i\varphi}\rangle_{b'} - \right. \\ \left. |-\beta \sin \frac{\varphi}{2}\rangle_a |\beta \cos \frac{\varphi}{2}\rangle_b |\gamma\rangle_{a'} |i\gamma e^{i\varphi}\rangle_{b'} \right) \quad (1)$$

where $\beta = \sqrt{T} \alpha e^{i\varphi/2}$ and $\gamma = \sqrt{R/2} \alpha$, a' and b' represent the loss mode of the two path. The density operator of this state is given by $\rho_{\text{out}} = |\psi\rangle_{\text{out}} \langle \psi|$, so that the output states of the MZI after tracing out the environment mode take the following form

$$\rho_{\text{out}} = |N_o|^2 \left(|\varepsilon\rangle_a |-\delta\rangle_{bb} \langle -\delta|_a \langle \varepsilon| + \right. \\ \left. |-\varepsilon\rangle_a |\delta\rangle_{bb} \langle \delta|_a \langle -\varepsilon| - e^{-2R|\alpha|^2} |\varepsilon\rangle_a |-\delta\rangle_{bb} \otimes \right. \\ \left. b \langle \delta|_a \langle -\varepsilon| - e^{-2R|\alpha|^2} |\varepsilon\rangle_a |-\delta\rangle_{bb} \langle -\delta|_a \langle \varepsilon| \right) \quad (2)$$

where $\varepsilon = \sqrt{T} \alpha \sin \frac{\varphi}{2} e^{i\varphi/2}$ and $\delta = \sqrt{T} \alpha \cos \frac{\varphi}{2} e^{i\varphi/2}$. It can be seen from Eq.(2) that photon loss suppresses the off-diagonal coherence between the two sensor states by a factor of $e^{-2R|\alpha|^2}$ and further destroys the expected performance of the system.

In the following we show that by substituting the intensity detection with a simple photon counting scheme with a post-binarization process, we beat the standard resolution limit and the shot noise limit in lossy and noisy environments.

2 Binary-outcomes parity photon counting measurement

Binary-outcome photon counting measurements are the common detection methods in the fields of quantum metrology and interferometry^[10-12]. Parity photon counting detection guarantees the optimal measurement of phase shift in optical interferometer in a wide range of non-classical input states of light. A general photon counting is described by a set of projection operators $\{|n, m\rangle\langle n, m|\}$ with the two-mode Fock states $|n, m\rangle = |n\rangle_a |m\rangle_b$. According to Eq.(2), the probability for detecting n photons at the output port a and m photons at the port b , i.e., coincidence rate $P(n, m|T, \varphi) = \langle n, m | \hat{\rho}_{\text{out}}(T, \varphi) | n, m \rangle$, is given by

$$P(n, m|T, \varphi) = 2|N_o|^2 \left\{ \left[e^{-T|\alpha|^2} \left(T|\alpha|^2 \sin^2 \frac{\varphi}{2} \right)^n \times \right. \right. \\ \left. \left(T|\alpha|^2 \cos^2 \frac{\varphi}{2} \right)^m - e^{-T|\alpha|^2 - 2R|\alpha|^2} \left(-T|\alpha|^2 \sin^2 \frac{\varphi}{2} \right)^n \times \right. \\ \left. \left. \left(-T|\alpha|^2 \cos^2 \frac{\varphi}{2} \right)^m \right] / n! m! \right\} \quad (3)$$

According to recent reports, there are two typical photon counting measurements, the parity detection and the zero-nonzero detection, and zero-nonzero photon counting gives better sensitivity than parity detection.

Parity detection was first proposed by Bollinger et al in the context of trapped ions in 1996, and later this detection was adopted for phase estimation by

Gerry. The parity detection, described by a parity operator $\hat{\Pi}_a = (-1)^{\hat{n}_a} = e^{i\pi \hat{a}^\dagger \hat{a}}$ at the output port a , divides the photon counting data $\{n, m\}$ into binary outcomes \pm , according to even or odd number of photons n at that output port. In other words, if n is an even number, $\Pi_a = +1$, otherwise $\Pi_a = -1$. According to Eq.(3), the probability for detecting n photons at the output port a can be obtained through summing over m , with its explicit form

$$P(n|T, \varphi) = 2|N_o|^2 e^{-T|\alpha|^2} \left[\left(T|\alpha|^2 \sin^2 \frac{\varphi}{2} \right) / n! \times e^{\frac{T|\alpha|^2 \cos^2 \frac{\varphi}{2}}{2}} - e^{-2R|\alpha|^2} e^{-\frac{T|\alpha|^2 \cos^2 \frac{\varphi}{2}}{2}} \left(-T|\alpha|^2 \sin^2 \frac{\varphi}{2} \right) / n! \right] \quad (4)$$

Through a sum of $P(n|T, \varphi)$ over the odd or the even number of n , the conditional probabilities $P(\pm|T, \varphi)$ can be obtained as

$$P(\pm) = \sum_{\text{odd or even } n} P(n|T, \varphi) = |N_o|^2 (1 \pm e^{-2T|\alpha|^2 \sin^2 \frac{\varphi}{2}} + e^{-2|\alpha|^2} \mp e^{-2T|\alpha|^2 \cos^2 \frac{\varphi}{2} - 2R|\alpha|^2}) \quad (5)$$

One can note that $P(+) + P(-) = 1$, and

$$\langle \hat{\Pi} \rangle = P(+) - P(-) = 2|N_o|^2 (e^{-2T|\alpha|^2 \sin^2 \frac{\varphi}{2}} - e^{-2R|\alpha|^2} e^{-2T|\alpha|^2 \cos^2 \frac{\varphi}{2}}) \quad (6)$$

Thus, from Eq.(6) it follows that the loss term $e^{-2R|\alpha|^2}$ just right erodes the coherence and further decays the detection performance.

2.1 Role of photon loss on the resolution and sensitivity

The theory and experiment of quantum interference with coherent states have already been detailed^[10-12]. However, in practical environments, the output performances of this kind interference are not the optimal at all. In the following section, the effects of loss on resolution and sensitivity have been analyzed based on above proposed scheme.

The resolution of the interference signal mainly depends on the types of light sources and detection schemes. In the absence of loss, the output signal of OCSS shows 2-fold super-resolving relative to that of CS, which is depicted in Fig.2 in solid line (the parity signal of OCSS) and in dot-dashed line (the

parity signal of CS). According to Refs. [8-9], resolution of parity measurement for coherent states is \sqrt{N} times improvement compared with the traditional intensity detection. Therefore, resolution for OCSS is $2\sqrt{N}$ times resolution enhancement relative to that of the traditional intensity signal (the blue dot-dashed line) of CS in the sense of the well-defined narrow feature, which has beaten the Rayleigh diffraction limit.

If the photon loss is taken into account, the situation will be different. Figure 2 shows the parity signal for OCSS in the case of $T=1$ (solid line), 0.99 (dashed line), 0.97 (dotted line) and 0.95 (dot-dashed line). It can be seen that 1% of the photon loss will make the interference pattern change markedly. Now, we define the peaks of the interference signal at the coordinates of $2k\pi$ ($k=0,1,2,\dots$) as the even interference peaks, and the rest peaks are referred to as the odd interference peaks.

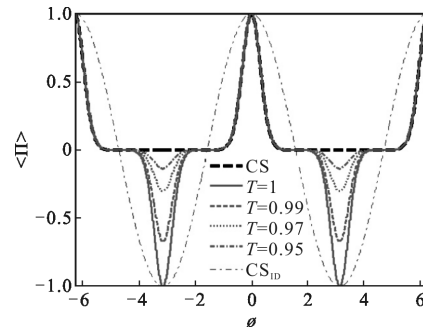


Fig.2 Expectation values $\langle \hat{\Pi} \rangle$ of Eq.(6) are plotted in lines against phase shift φ for an average power of $N=10$ in the absence and presence of loss, respectively.

Dot-dashed lines represent the normalized "classical" intensity difference signal and the dashed lines are the parity signals for CS. The solid, dashed, dotted and dot-dashed lines represent the cases of $T=1$, 0.99, 0.97 and 0.95, respectively

Then, photon loss greatly declines the amplitude of odd peaks and has no effects on that of even peaks. The rate of descent for the amplitude of odd peaks mainly depends on the lossy term $e^{-2R|\alpha|^2}$ of Eq.(6), in other words, the resolution of interferometric fringe

will be declining with the increasing loss rate R . If the resolution of interferometric fringe is represented as FWHM, then the average resolution can be expressed as

$$\overline{\Delta x} = \text{FWHM} / (1 + e^{-2R|\alpha|^2}) \quad (7)$$

From Eq. (7) we can see that the resolution depends on FWHM and R , while FWHM will also be affected by R . The fringe will be expanded with the increase of loss rate R , which can also be found in Fig.3. In much small loss regions (i.e., $0 < R < 0.2$), parity signal for OCSS (solid line) gives better resolution than that of CS (dashed line). However, in the rest loss regimes, resolution for OCSS is in agreement with that of CS.

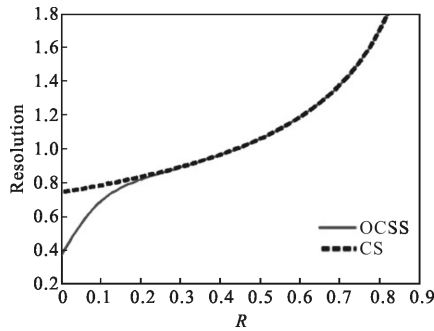


Fig.3 Resolution of parity photon counting measurements for OCSS and CS against loss rate R with $N=2$

Due to $\hat{\Pi}^2 = 1$, the Gaussian error -propagation formula gives the phase sensitivity:

$$\Delta\varphi = \sqrt{1 - \langle \hat{\Pi} \rangle^2} / d\langle \hat{\Pi} \rangle / d\varphi \quad (8)$$

The sensitivity for most interferometric signal is susceptible to loss and noise. In order to analyze the effects of loss on sensitivity, according to Eq.(6) and Eq.(8), we plot the minimum sensitive against R in solid curve in Fig.4 and the descending sensitivity with the increasing loss is obvious. The dashed line is the best sensitivity of CS with parity measurement. One can see that all lines merge with each other, which indicates the same effects of loss on all sensitivities. Therefore, the sensitivities of CS and OCSS are all at shot noise limit.

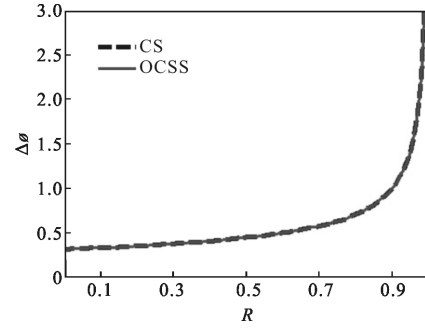


Fig.4 Best sensitivity of parity photon counting measurements for OCSS and CS against loss rate R with $N=16$

2.2 Effects of phase noise on resolution and sensitivity

The accumulated phase generated from the progress of light passing through the environment or media is a significant parameter for Lidar ranging. After phase accumulation, phase-diffusion process produces a phase noise $\Delta\varphi$ in one of the two paths (as depicted in Fig.1). Generally, the presence of phase noise can be modeled by the following master equation: $\partial \hat{\rho} / \partial t = \gamma(2\hat{N}\hat{\rho}\hat{N} - \hat{N}^2\hat{\rho} - \hat{\rho}\hat{N}^2)$ with $\hat{N} = \hat{a}^\dagger \hat{a}$ and the phase-diffusion rate γ . According to Refs.[15-16],

the solution of $\hat{\rho}$ is given by an integration $\hat{\rho}_\kappa \propto \int_R dx e^{-x^2/(4\kappa)} \hat{U}(x) \hat{\rho}(\varphi) \hat{U}^\dagger(x)$, where $\kappa = \gamma t$ is a dimensionless diffusion rate. Note that the phase-encoded state $\hat{\rho}(\varphi)$ obeys $\hat{U}(x) \hat{\rho}(\varphi) \hat{U}^\dagger(x) = \hat{\rho}(x + \varphi)$ for the noiseless case.

Replacing $x \rightarrow x - \varphi$, we obtain the final state

$$\hat{\rho}_{\kappa, \text{out}} = 1/\sqrt{4\pi\kappa} \int_R dx e^{-(x-\varphi)^2/4\kappa} \hat{\rho}_{\text{out}}(\varphi) \quad (9)$$

where $\hat{\rho}_{\text{out}}(\varphi)$ has been given by Eq. (2).

In the presence of the phase diffusion, all the relevant quantities can be obtained by integrating the Gaussian with the quantities without diffusion. For example, the binary-outcome parity photon counting measurement gives the output signal:

$$\langle \hat{\Pi} \rangle_\kappa = 1/\sqrt{4\pi\kappa} \int_R dx e^{-(x-\varphi)^2/4\kappa} \langle \hat{\Pi} \rangle \quad (10)$$

where $\langle \hat{\Pi} \rangle$ has been given by Eq.(6). Integrating it

with the Gaussian, we can obtain the exact numerical results of the resolution as a function of the diffusion rate κ depicted in Fig.5. The results indicated that all resolutions have decreased when the phase diffusion rate increases. However, the different changing tendency of resolution will be occurred in different diffusion region. In the diffusion region of $\kappa < 0.3$, OCSS gives the same resolution as that of CS. While in the rest regime, parity detection for OCSS (solid line) gives better resolution than that of CS (dashed line). In other words, the resolution of OCSS is much better than CS in large noise regimes.

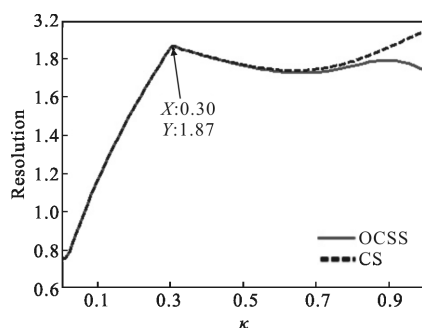


Fig.5 Resolution against phase diffusion rate κ with the average number of photon $N=10$

Similarly, according to Eq.(8) and Eq.(10), the numerical results of the sensitivity are illustrated in Fig.6. From Fig.6, it can be seen that the best

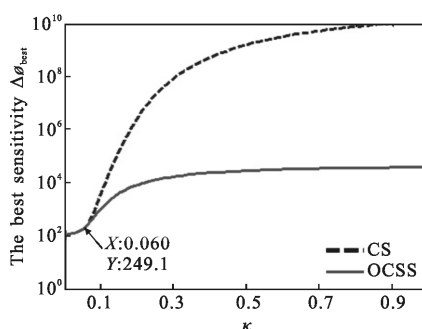


Fig.6 The best sensitivity against phase diffusion rate κ with the average number of photon $N=10$

sensitivity against phase noise of OCSS merges with that of CS in the diffusion regimes of $\kappa < 0.06$. However, in the diffusion regions of $\kappa > 0.06$, the best sensitivity of CS(dashed line) rapidly declines and the best sensitivity of OCSS slowly descends, that is to say that OCSS gives better sensitivity than that of CS.

3 Conclusion

In conclusion, the theory of lidar with new light sources has been investigated in practical environments. The odd coherent states with the characters of coherence and superposition have been adopted as the light source of lidar, and parity photon counting measurements are exploited to enhance its performances. Surprisingly, OCSS produces better resolution and sensitivity than CS under a certain conditions, especially in larger phase noise and smaller loss environments. More specifically, OCSS gives better resolution than CS in the lossy regions of $0 < R < 0.2$, and gives the same sensitivity as CS in the whole loss regimes. Taking the phase noise into account, OCSS performs better resolution and sensitivity in the regime of $\kappa > 0.3$ and $\kappa > 0.06$, respectively. In a word, in large noise environments, the performance of lidar with odd coherent superposition states light of sources are superior to the traditional lidar. Finally, our proposed scheme can be implemented in LADAR, especially in laser Doppler velocimetry.

References:

- [1] Caves C M. Quantum-mechanical noise in an interferometer [J]. *Phys Rev D*, 1981, 23: 1693.
- [2] Dowling, J P. Quantum optical metrology-the lowdown on high N00N states [J]. *Contemp Phys*, 2008, 49: 125.
- [3] Wang Q, Zhang Y, Xu Y, et al. Pseudorandom modulation quantum secured lidar [J]. *Optik-International Journal for Light and Electron Optics*, 2015, 126: 3344.
- [4] Wang Qiang, Zhang Yong, Hao Lili, et al. Super-resolving quantum LADAR with odd coherent superposition states sources at shot noise limit [J]. *Infrared and Laser Engineering*, 2015, 44(9): 2569. (in Chinese)
- [5] Boto A N, Kok P, Abrams D S, et al. Quantum interferometric optical lithography: exploiting entanglement to beat the diffraction limit[J]. *Phys Rev Lett*, 2000, 85: 2733.
- [6] Kok P, Lee H, Dowling J P. Creation of large-photon-number path entanglement conditioned on photodetection[J]. *Phys Rev A*, 2002, 65: 052104.
- [7] Sanders B C. Quantum dynamics of the nonlinear rotator and

- the effects of continual spin measurement [J]. *Phys Rev A*, 1989, 40: 2417.
- [8] Gao Y, Anisimov P M, Wildfeuer C F, et al. Super-resolution at the shot-noise limit with coherent states and photon-number-resolving detectors [J]. *J Opt Soc Am B*, 2010, 27: A170.
- [9] Jiang K, Lee H, Gerry C C, et al. Super-resolving quantum radar: Coherent-state sources with homodyne detection suffice to beat the diffraction limit [J]. *J Appl Phys*, 2013, 114: 193102.
- [10] Distant E, Ježek M, Andersen U L. Deterministic superresolution with coherent states at the shot noise limit[J]. *Phys Rev Lett*, 2013, 111: 033603.
- [11] Cohen L, Istrati D, Dovrat L, et al. Super-resolved phase measurements at the shot noise limit by parity measurement [J]. *Optics Express*, 2014, 22: 11945.
- [12] Feng X M, Jin G R, Yang W. Quantum interferometry with binary-outcome measurements in the presence of phase diffusion[J]. *Phys Rev A*, 2014, 90: 013807.
- [13] Glauber R J. Coherent and incoherent states of the radiation field[J]. *Phys Rev*, 1963, 131: 2766.
- [14] Dodonov V V, Malkin I A, Man'Ko V I. Even and odd coherent states and excitations of a singular oscillator [J]. *Physica*, 1974, 72: 597.
- [15] Brivio D, Cialdi S, Vezzoli S, et al. Experimental estimation of one-parameter qubit gates in the presence of phase diffusion[J]. *Phys Rev A*, 2010, 81: 012305.
- [16] Genoni M G, Olivares S, Brivio D, et al. Optical interferometry in the presence of large phase diffusion [J]. *Phys Rev A*, 2012, 85: 043817.